Cationic Copolymers of Norbornylized Seed Oils for Fiber-Reinforced Composite Applications

Jomin Thomas and Mark D. Soucek*

Read Online

ACCESS | Metrics & More | Article Recommendations | SI Supporting Information

ABSTRACT: Norbornylized seed oils, i.e., norbornylized linseed oil (NLO), norbornylized soybean oil (NSO), and norbornylized high oleic soybean oil (NHOSO), were synthesized via the Diels–Alder reaction of seed oil and dicyclopentadiene (DCPD) at high temperature (~235 °C) and high pressure (~80 psi), followed by cationic copolymerization using DCPD with boron trifluoride diethyl etherate catalyst. Norbornylized seed oils were characterized using H1 nuclear magnetic resonance (NMR), attenuated total reflectance-Fourier transform infrared, and gel permeation chromatography (GPC). Copolymers were formulated with four different DCPD contents, and curing was investigated using dynamic differential scanning calorimetry (DSC) measurements. It was found that the curing followed NLO > NSO > NHOSO with NLO having the highest exotherm, lowest activation energy, and lowest onset temperature. Furthermore, the gelation times were the least for NLO-DCPD copolymers. As anticipated, the degree of unsaturation and norbornene moieties strongly influenced the curing of copolymer thermosets. The copolymer products were compression-molded into thermosets and characterized by DSC, Soxhlet extraction, thermogravimetric analysis (TGA), H1 NMR, solid-state C13 NMR, and GPC. NLO-DCPD thermosets demonstrated high cure, higher thermal stability, glass transition temperature, and cross-linking capability compared to the other seed oil-DCPD counterparts. NMR and GPC results further suggested that bis-allylic and norbornene units concomitantly participated very actively during the cationic curing reaction. Moreover, scanning electron microscopy images of glass fiber-reinforced NLO-DCPD copolymer composites demonstrated good interfacial adhesion between the polymer matrix and fiber phases, imparting enhanced thermo-mechanical properties. This research opens a new venue for higher biobased greener polymer constituent for composite applications.
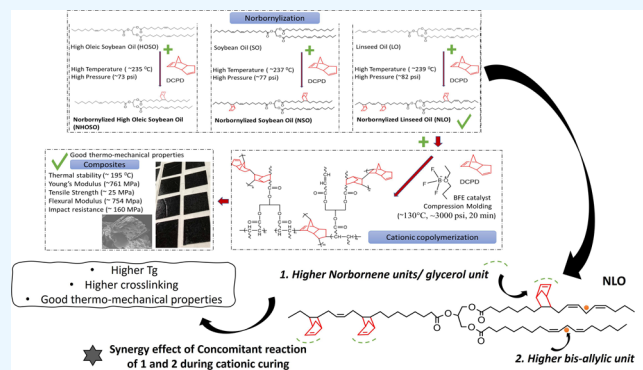
1. INTRODUCTION

Environmental impact of petroleum-based polymers has led to stringent environmental regulations,[1] and bioresourced green polymers[2,3] are in huge demand. Efforts are being made to study its degradation[4,5] and incorporate polymer recycling.[4] However, the most favorite route to polymer sustainability still remains the expanded use of renewable biobased resources.[6] Among the biobased polymers, the most common are those chiefly derived from starches, carbohydrates, and proteins.[3,7,8] However, vegetable oil has become a key "green" component as it can be a precursor for coatings, adhesives, plasticizers, and so forth.[9,10] Vegetable oil such as corn, soybean, linseed, castor, and tung oil has also been reported as comonomers in various reported research studies.[11–15] To that extent, linseed has been the most widely researched vegetable oil for a varied set of applications. It is attributed to its high degree of unsaturation present in the linseed oil, making it highly conducive to the copolymer synthesis, from brittle plastics to elastomers.[16,17] Even though soybeans are among the most common food crops in America, its easy availability and low cost have enabled its market expansion to coatings, plastics, and tire

industries.[18–23] High oleic soybean oil (HOSO) is yet another new and dynamic category of soybean oil that are essentially replacing partially hydrogenated oils, in various food and even nonfood industrial applications.[24] It is a genetically modified variant of soybean, finding its niche potential in industrial application like coatings, copolymers, asphalt plasticizer, and so forth.[25,26] Even so, the application of any of these seed oils in thermosets were limited until the last century.[27]

To that extent, functionalized vegetable oil with higher reactivity has a huge potential to overcome the inherent limitations.[13,28,29] There is a plethora of research carried out and numerous literature reported in functionalized vegetable oil.[30–32] Diels–Alder reaction between a dienophile and diene

is the most common synthetic route[33] for cyclic-ring systems. Norbornylization is such a reaction that incorporates norbornene rings to the vegetable oil chain, increasing its reactivity.[34] Previously reported work on functionalized vegetable oil includes electron transfer and Lewis acids catalyzed Diels–Alder reactions,[35,36] with Dilulin being one of the first commercial products containing norbornylized linseed oil (NLO).[37] Soucek and co-workers have reported the nobornylization of linseed oil[38] and soybean oil[39] and its subsequent epoxides, with potential usages in UV-curable coatings[34,40−42] and rubber plasticizer applications.[39,43]

Larock and co-workers have the most vast and meticulous study reported in the last few years, on curing of vegetable oil via thermal, free radical, cationic, and ring-opening metathesis polymerization.[30,44−48] Even though divinylbenzene (DVB) has been the most commonly reported comonomer in cationic polymerization of vegetable oil-based polymers,[49,50] dicyclopentadiene (DCPD) was chosen for our research. As compared to DVB, the abovementioned inexpensive DCPD effectively addresses the drawbacks of high cost and offers a simpler route to cure the previously DCPD-modified norbornylized oil. However, difference in reactivity between DCPD and seed oil has led to the use of Norway fish oil modifiers for better solubility effect to tackle the heterogeneity of the copolymers.[47,51] In this research, norbornylization of HOSO and the cationic copolymerization of the synthesized norbornylized seed oils using the boron trifluoride diethyl etherate (BFE) catalyst are reported for the first time. Furthermore, it negates the need for additional fish oil modifiers as the higher reactivity of norbornylized seed oils can form homogeneous copolymers as compared to conventional seed oils.

It is understood that polymers with good thermoset properties can be a precursor for polymer matrix composites (PMC),[52,53] which are used in automotive and wind turbine industry among many others.[51,54−56] Thus, in this research, linseed oil, soybean oil, and HOSO were utilized as precursors to study, compare, and investigate the effect of norbornylization, followed by cationic copolymerization. Furthermore, norbornylized seed oils as a precursor for thermoset and composite application is being reported here for the first time. We have been focused on conversion and modification of vegetable oils like linseed oil, soybean oil, and now HOSO, into industrially useful biopolymers. This is an effort to further expand the nonfood application of the synthesized biorenewable norbornylized seed oils. Representative thermosets and glass fiber-reinforced composites molded highlight their potential in composite applications. Thermo-mechanical properties and morphological evaluations serve to give an impetus to this research in the field of green chemistry and engineering.

2. EXPERIMENTAL SECTION

2.1. Materials. Dicyclopentadiene (Sigma-Aldrich), butylated hydroxy toluene (BHT), boron trifluoride diethyl etherate catalyst (BFE), and hexane were purchased from Sigma-Aldrich. Linseed oil and soybean oil of supreme grade were obtained from Cargill. HOSO was supplied by the Ohio Soybean Council (OSC). Chemical structures of the reacting constituents are provided in Figure 1.

2.2. Norbornylization. A slightly modified procedure from the previous work in Soucek's laboratory[38,42] was used for the norbornylization of linseed, soybean, and HOSO by Diels–
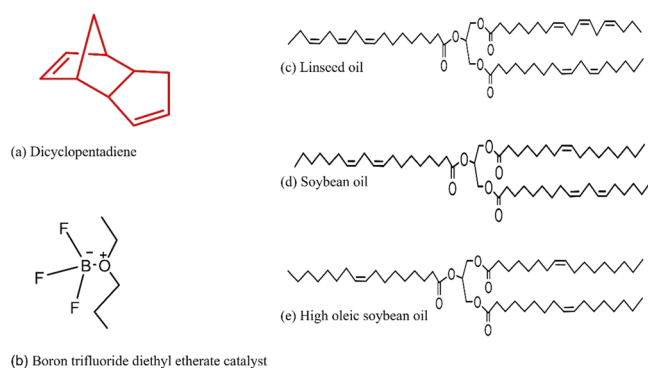
Figure 1. Structure of (a) dicyclopentadiene, (b) boron trifluoride diethyl etherate catalyst represent triglyceride unit fatty acid structures of (c) linseed oil, (d) soybean oil, and (e) high oleic soybean oil.

Alder reaction. A mole ratio of 1.5 (ratio of DCPD/C=C of the corresponding oil) was chosen as it enabled the highest level of norbornylization, as reported in the previous work from Soucek's laboratory.[38,39] The process parameters like temperature, pressure, and torque were carefully monitored for each reaction.

2.3. Cationic Polymerization. Preweighed amounts of NLO/NSO/NHOSO and DCPD (97 wt % total) were mixed in a 200 mL beaker and was stirred vigorously at room temperature until a homogeneous solution was obtained. Within the 97% mixture, varying concentrations of DCPD loadings, 0, 20, 40, and 60 wt % was experimented on. It was followed by the dropwise addition of 3 wt % BFE catalyst into the mixture. The reaction mixture was stirred vigorously until it became homogeneous and was taken out of the beaker for the next stage. Cure study of the copolymer was carried out by multiple dynamic differential scanning calorimetry (DSC) scans.

2.4. Thermoset Processing and Composite Fabrication. The NLO-DCPD, NSO-DCPD, and NHOSO-DCPD copolymers were further utilized to mold thermosets and composites. The carver press compression molder was utilized for molding. The mold was preheated to 130 °C, and premix was poured onto the mold. A mold of dimension 5″ × 5″ × 1/8″ was used, which required 40 g of the premix. It was compression-molded for 30 min at 130 °C at a pressure of about 3000 psi. Next, it was cold-pressed for 10 min and was taken out of the mold. Thermo-mechanical properties were investigated, and the best copolymer system suitable for a thermoset was shortlisted. The molding process conditions of thermosets remained the same for composites, except for a layer of random oriented glass fiber cut to the shape of the mold and placed at the start. The formulation was adjusted to 70% copolymer mixture and 30% fiber glass reinforcement by weight.

2.5. Characterization and Testing. A Brookfield DV II+ Pro viscometer was used to measure viscosity of norbornylized oil at a 20 rpm setting at 22 °C using the LV Spindle. IR spectra were collected on a Thermo Scientific Nicolet iS50 FTIR spectrometer with a diamond ATR module with a 4 cm^{-1} resolution and 128 co-added scans. Data acquisitions were performed using Omnic FT-IR software (Nicolet). The cure behavior of the norbornylized oil with 0−60 wt % DCPD loadings were examined using dynamic scans in DSC Q2000 from TA instruments. A sample of 5−10 mg was loaded into Tzero aluminum hermetic pans and placed into the DSC cell,

which was precooled to −40 °C. Samples were heated from 0 to 220 °C at rates of 5, 10, and 20 °C min⁻¹ under a steady nitrogen purge flow of 40 mL/min.

Soxhlet extractions data were utilized for information about the degree of cross-linking of the thermosets, giving the percentage of insoluble and soluble content in the bulk copolymer thermosets. For Soxhlet extractions, 2−4 g of the bulk polymer sample was extracted for 24 h with 100 mL of methylene chloride using a Soxhlet extractor. Subsequently, the solution in the distillation pot was concentrated under reduced pressure and dried overnight at 60 °C in a vacuum oven. Prior to weighing, both the resulting soluble portion in the pot and recovered insoluble portion was dried under a vacuum. The soluble portion after the extraction was evaluated with nuclear magnetic resonance (NMR) and gel permeation chromatography (GPC). Insoluble extracts of the cross-linked bulk copolymer were evaluated by solid-state C13 NMR. Gelation times were determined by measuring the time required for the liquid reactants to reach a nonpourable viscosity, beyond which point, it has no processability. ASTM D2471-99 standard was followed, and five individual measurements were taken and averaged at a certain temperature.

H1 NMR spectra were recorded on a VARIAN Inova 500 GHz spectrometer using CDCl₃ as a solvent and tetramethyl silane as a standard. It was referenced using deuterated solvent shifts (CHCl3 δ = 7.26 ppm). Data analysis of the spectra was carried out on the ACD-NMR software. Tosoh EcoSEC HLC-8320 GPC was used to find the molecular weight and polydispersity index of all the norbornylized oil. It had an RI detector with two 17, 393 TSK gel columns (7.8 mm ID × 30 cm, 13 μm) and one 17367-TSK gel Guard Column (7.5 mm ID × 7.5 cm, 13 μm). Inhibitor-free high-performance liquid chromatography (HPLC)-grade tetrahydrofuran (THF) was used as the eluent at an injection volume of 80 μL and a flow rate of 1 mL/min at 40 °C. The obtained data were measured relative to the polystyrene standards, which were calibrated less than 4 months prior to data collection.

Solid-state cross-polarization/magic angle spinning (CP/MAS) NMR spectra were measured on an Agilent NMRS 500 spectrometer at 125.6 MHz for 13C using a 4 mm T3HXY probe. The samples were crushed with a mortar and pestle, packed into 4 mm zirconia rotors with a Kel-F dive tip and PVDF end cap and spacers. The rotors were spun at 12 kHz ± 5 Hz. The spectra were obtained using a 5 s recycle delay, 0.015 s acquisition time, a 50 kHz spectral window, a 4 μs 1H 90° pulse, a 62.5 kHz linear-ramped cross-polarization field, 1.4 ms contact time, and 62.5 kHz SPINAL decoupling. 13C chemical shifts were referenced to the hexamethylbenzene methyl resonance assigned at δ 17.3 ppm. The spectra were processed with 50 Hz exponential line broadening and zero-filled to 4096 points. Data analysis of the spectra was carried out on the ACD-NMR software.

Dynamic mechanical analysis (DMA) was performed with TA Q800 on samples with a rectangular dimension of 30 × 10 ×1 mm³ (length × width × thickness). The damping factor (tan δ) and elastic modulus (E') were collected at 3 °C/min heating rate at a range of 25−200 °C and 1.0 Hz frequency. The DMA was operated under the tension mode. The TGA instrument (TA Q500) was used to probe the thermal stability of thermosets from room temperature to 600 °C at a scanning rate of 20 °C/min with a sample weight of about 10 mg. The test was carried out under nitrogen, as the sample purge gas. $T_{5\%}$, $T_{30\%}$, T_{max}, and T_s were used as the parameters to study

and compare the thermal stabilities of the thermosets and composites. $T_{5\%}$ signifies the temperature at which 5 wt % of the material has degraded, and T_{max} is the temperature where the maximum degradation of the composite occurs, which is known as the thermal decomposition temperature.[57] Furthermore, the statistic heat-resistant index temperature (T_s) is a characteristic aspect of thermal stability and was calculated according to eq 1.

$$T_s = 0.49 \times [T_{5\%} + 0.6 \times (T_{30\%} - T_{5\%})] \tag{1}$$

Mechanical properties of the composites were evaluated by tensile, flexural, and impact measurements. The tensile properties were examined at room temperature on an Instron 5540 universal testing machine according to ASTM D3039. A load cell of 10 KN at a 50 mm/min cross-head rate was used as the testing condition. Stress−strain curves were plotted using the Instron machine readings to calculate all the pertinent values like Young's modulus, tensile strength, and toughness. Young's modulus is the linear region (Rise/run) relevant to the stress vs strain curve, and the stress point just before the sample breaks is the ultimate tensile strength. The area under the stress−strain curve is the toughness. The tests were performed on rectangular samples (120 × 15 × 3 mm) cut out from the composite using sharp sample cutters, with the gauge length kept constant at 50 mm. Flexural tests were performed by Instron 5540 universal testing machine under the three-point bending mode at a strain rate of 0.01 mm/mm/min according to ASTM D790 (Type I method using cross-head position). Flexural modulus and flexural strength of the composites were evaluated. Samples had a rectangular dimension of 125 × 12.75 × 3 mm³, and the span length was kept constant at 50 mm. Impact testing was carried out on Instron CEAST 9050 equipment according to the ASTM D4812, Izod testing with a hammer/pendulum of 5.5 J. Samples had a rectangular dimension of 62 × 12.75 × 3 mm³. The impact properties were evaluated majorly in terms of impact strength as the average impact resistance (J/m) of the specimen. All test results are the average value of five specimens, and the standard deviations were calculated and marked.

The morphological study of fracture surfaces was obtained at a magnification of 250× and 500× using a LYRA 3 TESCAN scanning electron microscope (SEM) instrument. The fractured surfaces of the tensile specimens were mounted vertically on a sample holder to expose the composite's cross-section. The samples were sputter-coated with a platinum layer before examination. A 5 kV beam was used, and secondary electron images were collected.

3. RESULTS AND DISCUSSION

3.1. Norbornylization. The process of norbornylization involves the incorporation of norbornene units into the oil fatty acid backbone using a Diels−Alder reaction. It is a [4 + 2] cycloaddition reaction between a diene and dienophile, (cyclopentadiene and oil, respectively, in this case), forming cyclic molecules[58] (Supporting information, Scheme S1). The concept was first commercialized by Cargill, introducing Dilulin, DCPD-modified linseed oil into the market. Larock and co-workers studied Dilulin and its cationic and Ring Opening Metathesis Polymerization (ROMP) reactions in depth,[59] whereas Soucek and co-workers concentrated on the synthesis, characterization, and application of similar norbor-
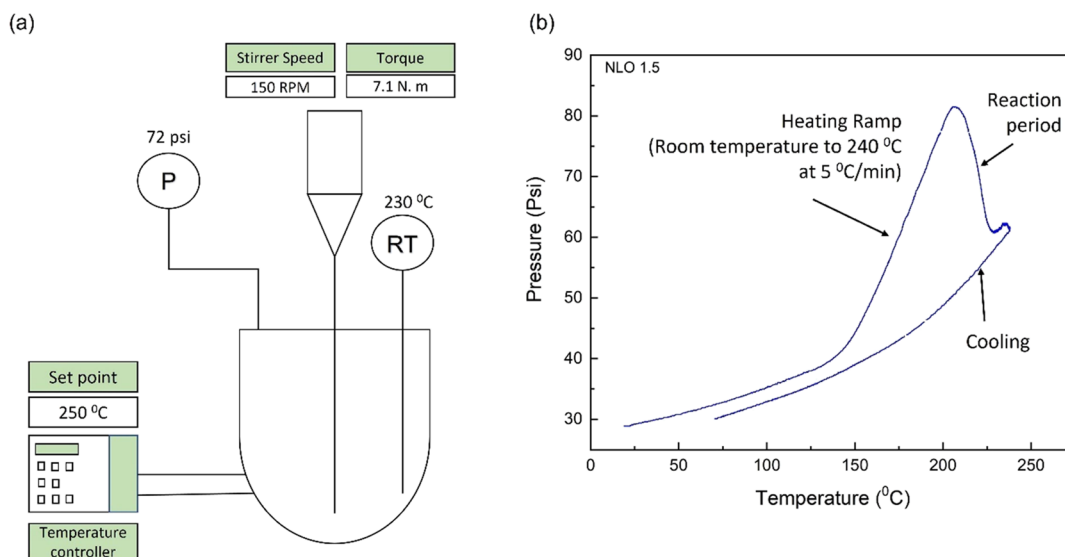
Figure 2. (a) Schematics of the HEL reactor and (b) reactor pressure as a function of reactor temperature: NLO batches.

nylized linseed and soybean oil with higher levels of norbornylization compared to the commercial standard.[38,39]

In addition to the NLO and NSO already reported, herein, we report the norbornylization of HOSO for the first time. High temperature to facilitate the carbon−carbon double bond activation in oil, coupled with the high pressurized reaction to enhance the cyclopentadiene solubility in the oil, proved to be an efficient way for nobornylization. A thorough study of the pressure dynamics in the HEL reactor of nobornylization batches were carried out. A plot of pressure versus temperature, Figure 2, reveals that pressure increases when DCPD is near its boiling point (170 °C), and it follows a hysteresis loop. DCPD cracks into cyclopentadiene units around that temperature range and reaction progresses. As the reaction is held above 200 °C for 2 h and subsequently cooled down, it retraces the initial pressure as closely. The maximum pressure attained during nobornylization varied with the different oil used. NLO-1.5 showed the highest pressure (82 psi) and NHOSO 1.5 showed the lowest (72 psi).

GPC chromatograms were used for evaluating the molecular weight and polydispersity index (Supporting information Figure S1). The main peak is of norbornylized oil. The small step peak to the right can be attributed to the residual cyclopentadiene oligomers (Mw ∼ 260), as per similar retention time for DCPD GPC conducted for comparison purpose. NLO-1.5 was a soft liquid with very high viscosity. NHOSO-1.5, however, exhibited relatively lower viscosity. It can be attributed to the difference in the molecular weight of the norbornylized oil. An average molecular weight of 1420 g/mol was observed in the GPC chromatogram of NHOSO, whereas NSO and NLO showed 1470 and 1560 g/mol, respectively. The physical properties of norbornylization batches are tabulated in Table 1. In the case of non-norbornylized oil, the GPC chromatogram shows one major oil peak at a specified retention time. However, once the seed oils are norbornylized, it consists of a majority of norbornylized seed oils, with unreacted non-norbornylized oil oligomers and cyclopentadiene oligomers. Only the relevant retention time peak was tabulated in Table 1. Thus, a direct point-to-point correlation with the viscosity of non-norbornylized and norbornylized seed oil is not feasible. The norbornylized

Table 1. Physical Properties of Norbornylized Seed Oil (NLO, NSO and NHOSO)

	pressure (psi)	viscosity (mPa s)	Mw: (g/mol)	Mn: (g/mol)	PDI
HOSO		1620	1411	1287	1.096
NHOSO-1.5	72.5	12,057	1424	1299	1.098
SO		1860	1397	1272	1.098
NSO-1.5	77	24,925	1475	1324	1.114
LO		1020	1317	1203	1.095
NLO-1.5	81.5	>30,000	1605	1428	1.124

seed oil chromatogram also shows the peaks for unreacted non-norbornylized oil oligomers and cyclopentadiene oligomers. Please refer to the GPC chromatograms provided in the Supporting Information Figure S1 for more detail or the previous work by Chen et al. for ESI-MS.[38]

FTIR spectra is provided in the Supporting Information Figure S2. There were no changes observed in the spectra for NHOSO and followed the same trend as our reported work with noborornylization of linseed oil[38] and soybean oil.[39,42] The band at 3007 cm^{-1} was attributed to the C−H stretching of oil C═C−H, whose intensity decreased after nobornylization. A new band at 3052 cm^{-1} appeared in the spectra of norbornylized oil, which is attributed to the C−H stretching of norbornene. The degree of unsaturation, nobornylization, and the percentage of cyclopentadiene oligomers formed are calculated as stated in Supporting information Section S1. Table 2 shows the major fatty acid compositions and degree of unsaturation of linseed oil, soybean oil, and HOSO (calculated experimentally and obtained from the literature).

Scheme 1 summarizes the process of norbornylization and some of the physical properties for NHOSO, NLO, and NSO. Nobornylization (43%) was achieved in NLO. Analogous NSO and NHOSO had a lower level of nobornylization with lower viscosity and molecular weight. Higher norbornylization in NLO can be attributed to the higher degree of unsaturation present in linseed oil. Furthermore, the higher molecular weight and viscosity of NLO can also be attributed to the chemical structure of the norbornylized constituents, with higher number of norbornene units incorporated into the backbone, as shown in the Scheme 1.

Table 2. Fatty Acid Compositions and Degree of Unsaturation of Linseed Oil, Soybean Oil, and High Oleic Soybean Oil[a]

natural oil	oleic acid (%) C18:1	linoleic acid (%) C18:2	linolenic acid (%) C18:3	degree of unsaturation (average C=C per triglyceride unit of oil)
linseed oil	19	24	47	6.36 (5.9)
soybean oil	23	54	8	4.1 (4.5)
high oleic soybean oil	76	6.7	2	3.02 (3.1)

[a]Only the three major fatty acids were included. Oils also contain saturated fatty acids like palmitic, stearic acids, and so forth. The values in parenthesis shows the reported values in the literature, whereas outer values are calculated by H1 NMR experimentally adapted in part with permission from ref 60, Copyright [2006] American Chemical Society.

Thus, there are 1, 2, and 3 norbornene units per triglyceride unit of NHOSO, NSO, and NLO, respectively, as evidenced by H1 NMR results. However, LO and SO with a higher degree of unsaturation per triglyceride unit (6.2 and 4.3, respectively), there is also the possibility of oligomerization. It can happen in anaerobic conditions in the reactor, leading to bodied oil or via autoxidation in the aerobic conditions (blown oil).[64] However, no oil oligomerization was observed in the GPC chromatograms (Supporting Section S.2). Instead, cyclopentadiene oligomerization was observed. Even though butylated hydroxytoluene (4 wt % DCPD) was included in the formation as a free radical retarder to inhibit the homopolymerization of cyclopentadiene, a certain amount of cyclopentadiene oligomerization (~8%) was still observed in all norbornylized oil. Compared to the carbon−carbon double in the oil, the conjugation in cyclopentadiene is more reactive and can result in the latter's homopolymerization.[38]

3.2. Cationic Copolymerization. It is critical that we look at the characteristics of norbornylized and dicyclopentadiene as cationic monomers using the BFE catalyst. The in-depth concept of cationic polymerization of soybean oil and DCPD has been reported.[30,47,51,59] In short, the decrease in entropy caused by loss of translational degrees of freedom of triglycerides makes thermodynamic feasibility depend entirely on the reaction being sufficiently exothermic. Carbon−carbon double bonds of seed oils are sites for electrophilic attack via reactive species generated by the BFE catalyst, and these reactions are exothermic. Thus, norbornylized seed oils are sufficiently nucleophilic and can polymerize cationically by the addition of monomers to the growing carbocation chain.[65] However, homopolymerization can lead to viscous fluids of very limited use. Therefore, it is necessary that it was copolymerized with a rigid comonomer like styrene, divinyl benzene, or dicyclopentadiene. This copolymerization also helps in enhanced mechanical and thermal properties.[7,11] Moreover, the high reactivity of the strained norbornene ring and higher degree of unsaturation make norbornylized seed oil advantageous to highly cross-linked networks via cationic polymerization with DCPD and BFE catalyst. Furthermore, norbornylization of seed oil also increases the reactivity significantly and eliminates the need for NFE-catalyst usage, which is otherwise commonly employed for achieving homogenous copolymers.[59−63]

Next, DCPD as the cross-linker needs to be investigated in a comprehensive manner owing to its features. DCPD was selected as the cross-linker for its rigid bicyclic structure. Known as the Diels−Alder dimer of cyclopentadiene, DCPD is widely used as a comonomer in EPDM elastomers, polyester and alkyd diluents, adhesives, floor coverings, and textiles.[66] A significant research data and microstructure elucidation are available for cationic DCPD polymers.[11,30,59,67] The characteristic of DCPD having two carbon−carbon double bonds of different reactivity (norbornyl and cyclopentadienyl double bond) has always been an interesting research topic. It is elucidated by several reported literature that norbornyl double bonds are more prominent and reactive among the structural units incorporated into the cationic poly dicyclopentadiene (polyDCPD) backbone.[68,69] Supporting information Scheme S2 shows the different DCPD structural units possible during the cationic polymerization of DCPD. The location of the electrophilic attack determines various DCPD structural units in the copolymers. If the electrophile attacks on norbornyl double bonds, it leads to an endo-unit, which can further rearrange to give an exo-unit.[68] It has been reported by Rule et

Scheme 1. Reaction Pathway of Norbornylization of Linseed, Soybean, and High Oleic Soybean Oil and Summary of Its Physical Characteristics

High Oleic Soybean Oil (HOSO)

High Temperature (~235 °C)
High Pressure (~73 psi)

DCPD

Norbornylized High Oleic Soybean Oil (NHOSO)
1. Molar ratio of DCPD/C=C (**1.5**)
2. Molecular weight (**1299 g/mol**)
3. Viscosity (**12057 mPa.s**)
4. Norbornylization (**27%**)
5. DCPD Wt.% in formulation (**25.2%**)
6. CPD Oligomerization (**8%**)

Soybean Oil (SO)

High Temperature (~237 °C)
High Pressure (~77 psi)

DCPD

Norbornylized Soybean Oil (NSO)
1. Molar ratio of DCPD/C=C (**1.5**)
2. Molecular weight (**1324 g/mol**)
3. Viscosity (**24925 mPa.s**)
4. Norbornylization (**33%**)
5. DCPD Wt.% in formulation (**32.7%**)
6. CPD Oligomerization (**8.3%**)

Linseed Oil (LO)

High Temperature (~239 °C)
High Pressure (~82 psi)

DCPD

Norbornylized Linseed Oil (NLO)
1. Molar ratio of DCPD/C=C (**1.5**)
2. Molecular weight (**1428 g/mol**)
3. Viscosity (**> 30,000 mPa.s**)
4. Norbornylization (**43%**)
5. DCPD Wt.% in formulation (**42.3%**)
6. CPD Oligomerization (**8.5%**)

2. Measured by GPC, 3. Measured by Brookfield viscometer
4 and 6 calculated by NMR, Resonance 5.9-6.01 ppm (Norbornene) and 5.6 ppm (Cyclopentadiene)
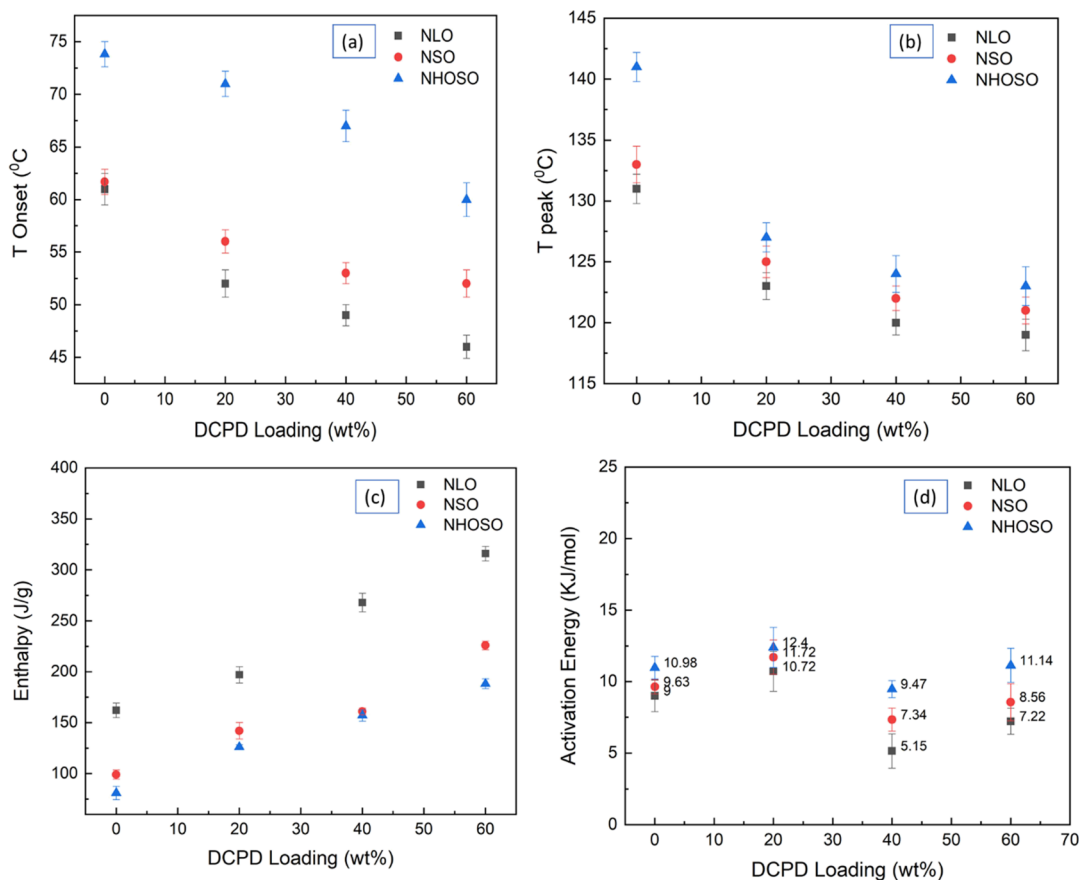
Figure 3. DSC cure study of NLO, NSO, and NHOSO. (a) Onset temperature, (b) peak temperature, (c) enthalpy, and (d) activation energy as a function of DCPD loading.

al. that exo-DCPD is more energetically favored and stable than endo-DCPD.[69] Furthermore, some researchers have also polymerized DCPD with a Ti-based initiator and found that electrophilic attack on cyclopentyl double bonds leads to units 3 and 4.[70,71] The propagation stage of the intermediates determines the final DCPD structural unit (Supporting information Scheme S2).[68]

DSC measurements are critical in determining the optimum temperature of thermoset molding via a compression mold. The DSC data table summarized from the curves used for the analysis are provided in the Supporting Information Section S2. The cationic cure of the norbornylized oil and DCPD was characterized by a broad exothermic peak in the DSC measurements. Heterogenous nature of the copolymer formed is observed as a small step in some of the formulations because of difference in reactivity between norbornylized oil and DCPD. Values of activation energy (E_a) for all the NVO batches were determined using the Kissinger's equation[72] as given in eq 2.

$$\ln\left(\frac{\beta}{T_P^2}\right) = \frac{-E_a}{RT_p} + \ln\left(\frac{AR}{E_a}\right) \tag{2}$$

where T_p is the peak temperature of the corresponding dynamic cure exotherm and β is the heating rate. E_a is calculated from the slope of a linear regression of the plot of $\ln\left(\frac{\beta}{T_P^2}\right)$ as a function of $1/T_p$ (Figure 3). It was observed during the cure study that both peak and onset temperatures

are found to decrease with increasing DCPD content, indicating an increase in cure. Furthermore, with the increase in DCPD loading, total enthalpy of the reaction was increased. When comparing between NHOSO, NSO, and NLO; onset and peak temperature decreased, whereas the enthalpy increased. This demonstrates a higher cure in NLO, closely followed by NSO and NHOSO. Furthermore, a similar systematic dependence of activation energy as a function of DCPD loading or norbornylization was also observed. NLO batches demonstrated the lowest activation energy whereas NHOSO exhibited the maximum. However, shifts from this trend were observed in some of the early formulation with more seed oil content and lesser DCPD. This observation can be attributed to the complexity of seed oil containing varying concentrations of fatty acids. With the addition of more DCPD content, there was a clear trend of increasing activation energy in the order of NLO < NSO < NHOSO. Lower activation energy translates to higher reactivity of the copolymer, and DSC characterization studies show the cationic curing is in the order NLO > NSO < NHOSO.

3.3. Thermoset Characterization and Properties. The fully cured norbornylized-DCPD copolymers were all obtained in quantitative yield essentially and appear as brown materials at room temperature. NHOSO−DCPD copolymers tend to be rubbery in nature, whereas the NLO-DCPD copolymers were tough and ductile materials. These copolymer thermosets were further studied by Soxhlet extraction with methylene chloride as the refluxing solvent. The purpose was to understand the

degree of the cross-linking efficiency in the thermosets molded and the bulk copolymer constituents.

Table 3 summarizes the results obtained by Soxhlet extraction. Typically, after 24 h Soxhlet extraction, 31−42,

Table 3. Gelation Times and Soxhlet Extraction Data for NLO/NSO/NHOSO DCPD Copolymers

NVO-R-DCPD copolymers	Soxhlet extraction data (%)		gelation times (min)
	insoluble	soluble	
NHOSO-DCPD-20	42	58	45
NHOSO-DCPD-40	39	61	34
NHOSO-DCPD-60	31	69	37
NSO-DCPD-20	52	48	17
NSO-DCPD-40	49	51	15
NSO-DCPD-60	43	57	14
NLO-DCPD-20	**67**	**33**	**10**
NLO-DCPD-40	**74**	**26**	**12**
NLO-DCPD-60	**79**	**21**	**8**

43−52, and 67−79 wt % insoluble materials were retained from the NHOSO, NSO, and NLO DCPD copolymers, respectively. Because of the higher cure efficiency of the NLOs, the yield of the cross-linked materials from NLO-DCPD copolymers were noticeably higher than that of the corresponding NSO and NHOSO systems. Thus, NLO-DCPD yielded copolymer thermosets of better cross-linking efficiency. Gelation times were measured at 80 °C because NHOSO batches failed to gel at room temperature or 50 °C, even after 24 h. Our results indicate that NLO-DCPD copolymers had shorter gelation times than other copolymers, presumably due to the higher cure efficiency of NLO during the cationic copolymerization. The much higher gelation time of NHOSO-DCPD copolymers can be a direct consequence of the low cure efficiency exhibited by NHOSO comparatively. However, a similar systematic dependence of DCPD incorporation on the gelation times were not observed.

Soluble extracts evaluated by GPC and NMR and solid-state C13 NMR of insoluble extracts were utilized for understanding

their molecular structure formation. GPC analysis confirms that the molecular weights of the soluble extracts range from 200 to 32,000 g/mol based on polystyrene standards. Supporting information Section S3 shows a series of GPC chromatograms of soluble extracts of norbornylized seed oil-DCPD copolymers with the interpretation of data. The GPC data confirm that there is presence of soluble components relating to NLO-DCPD oligomers along with DCPD oligomers and fatty acid fractions.

H1 NMR spectral analyses were carried out to further confirm the prospective chemical structure of the soluble extracts. Figure 4 (and Supporting Information Figure S3) shows the spectra corresponding to the NLO-DCPD soluble extracts. DCPD, LO, and NLO spectra were also provided for comparison purposes. The presence of linseed oil was evidenced by resonance at δ 4.1−4.4 ppm in LO and NLO, corresponding to the protons of the glycerol unit in the oil. It corroborates the observation of GPC, confirming the presence of unreacted oil in the soluble extracts. The absence of resonance at δ 5.95−6.0 ppm, corresponding to the proton of the norbornene unit, clearly indicates that the norbornene units are reacted during cationic copolymerization. However, resonance δ 5.6 ppm shows that there might be presence of cyclopentadiene oligomers in the soluble extracts, with their intensity increasing gradually as the DCPD content increases in the formulation. It shows that the cyclopentadiene moieties are a direct consequence of the DCPD addition and can form effective cross-links in the bulk materials. Thus, there are possibilities of soluble cross-linked materials, plasticized by the soluble oil components.

Two other interesting and key observations can be derived from the cured soluble extract H1 NMR spectrum (Figure 4): the disappearance of bis-allylic proton resonance at δ 2.8 ppm suggests the concurrent reaction of the reactive bis-allylic units of the NLO in the cationic curing process, and the new resonances at δ 5.45 and δ 5.5 ppm represent the endo-unit and the exo-unit of DCPD, showing evidence for the structure proposed in Scheme 2. Solid-state C13 NMR of the insoluble extracts were carried out to confirm the incorporation of DCPD units and NLO into the cross-linked polymer network
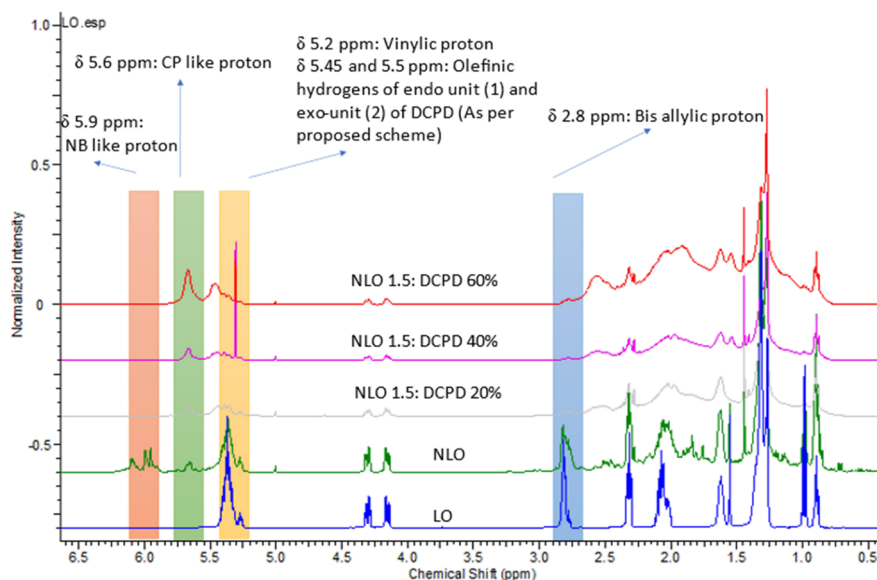
Figure 4. H1 NMR spectra of the NLO-DCPD copolymer soluble extracts after Soxhlet extractions.

Scheme 2. Cationic Copolymerization of NLO and DCPD
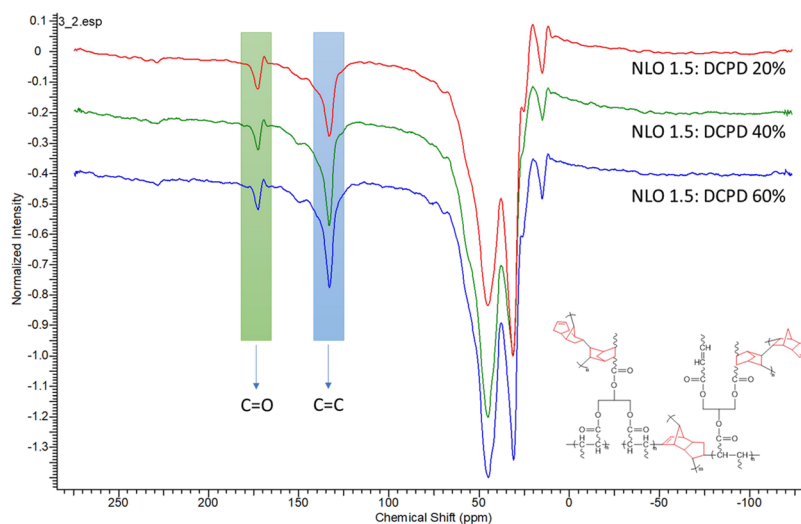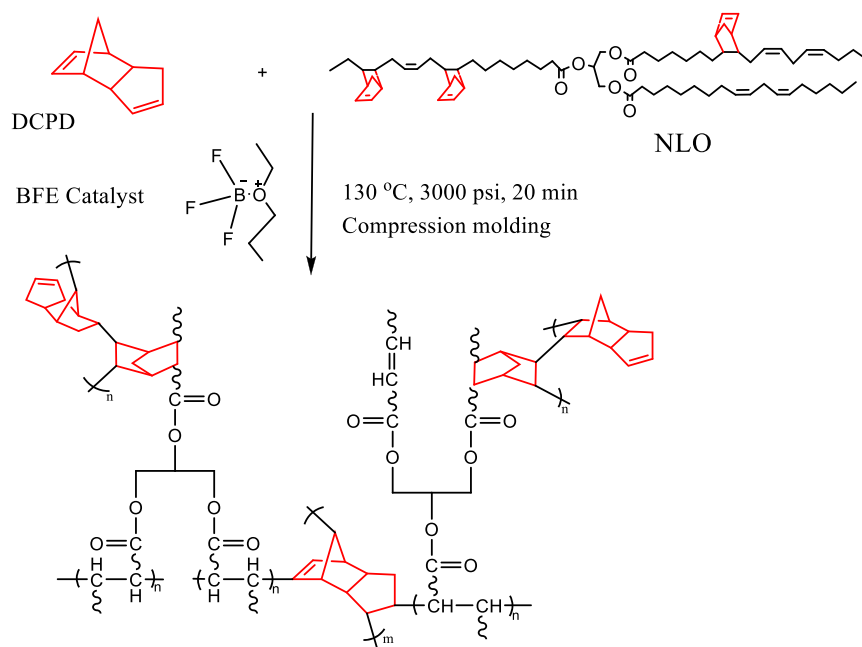
Figure 5. Solid-state C13 NMR spectra of NLO-DCPD copolymer insoluble materials after Soxhlet extraction.

(Figure 5). Resonances of C=O at δ 170 ppm and C=C at δ 130 ppm indicates the inclusion of oil and DCPD units into the bulk copolymer.[47] As observed from Figure 5, cross-linked NLO-DCPD 20 is different from that of NLO-DCPD-60. This observation substantiates that there can be a lower amount of unreacted soy and soluble components in NLO-DCPD-60. Furthermore, it translates to more homogenous cross-linked NLO-DCPD-60 bulk copolymer with increased Tg, as evidenced by the higher intensity of corresponding DCPD units at resonance δ 130 ppm.

Dynamic DSC scans of the fully cured material were used to evaluate the glass transition temperature of the thermosets. The glass transition temperature of the thermosets increased with the increase in the DCPD content, as shown in the Figure 6. Rigid bicyclic units of DCPD increases the glass transition temperature of the bulk copolymers. Furthermore, among the norbornylized seed oil-based DCPD copolymers, NLO copolymers showed the highest T_g, followed by NSO and

NHOSO copolymers. This observation corroborates the fact that LO has the highest unsaturation followed by SO and HOSO and thus has more reactive norbornene groups incorporated into the oil backbone, as was seen from the DSC characterization study. HOSO has more flexible triglyceride units, which is incorporated into the cross-linked structure, resulting in a thermoset with lesser T_g, as compared to LO or SO-based thermosets. All the values pertinent to a particular series were similar, covering a small range of difference. For instance, all the T_g values range between 50 and 60 °C.

TGA of the thermosets reveals that it was thermally stable up to 200 °C. The thermograms are provided in the Supporting Information Figure S4. All of them exhibit two-stage thermal degradation. The first stage can be attributed to the evaporation and decomposition of the soluble components in the bulk materials and unreacted oil (200−460 °C). The second stage corresponds to the degradation of the cross-
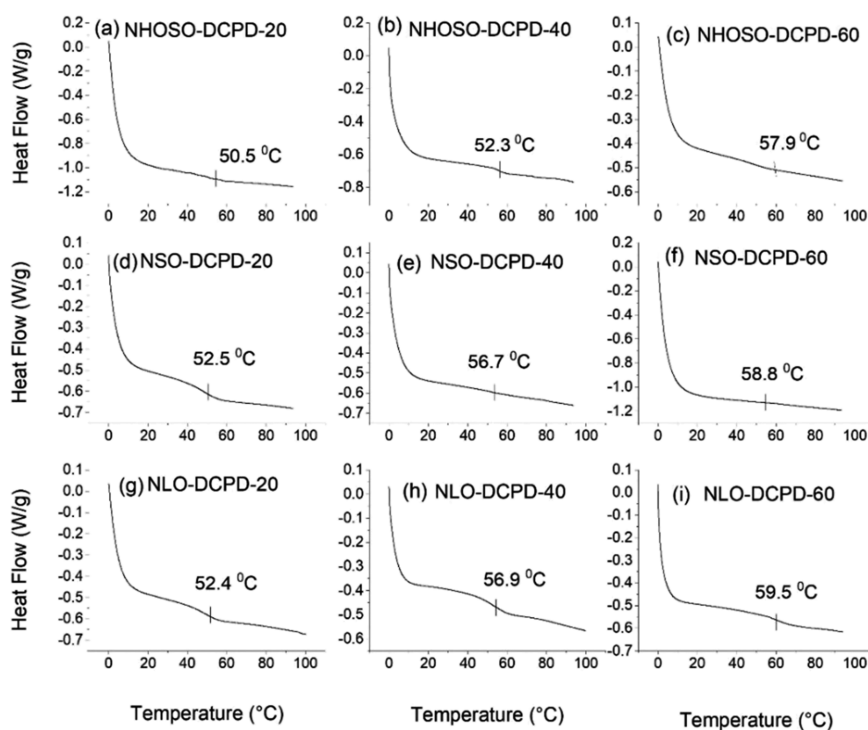
Figure 6. DSC thermogram of norbornylized seed oil-DCPD thermosets showing the T_g (a) NHOSO-DCPD-20, (b) NHOSO-DCPD-40, (c) NHOSO-DCPD-60, (d) NSO-DCPD-20, (E) NSO-DCPD-40, (f) NSO-DCPD-60, (g) NLO-DCPD-20, (h) NLO-DCPD-40, and (i) NLO-DCPD-60.

linked polymer structure and is the fastest degradation stage (450−500 °C). As observed from the GPC and H1 NMR of the soluble extracts, this stage can be attributed to both the unreacted oil components and the DCPD-based bulk polymer soluble fractions mentioned earlier. The char/residue content increases as the DCPD content in the copolymer formulation increases. Thermal properties of the NLO/NSO/NHOSO-DCPD thermosets are summarized in Table 4.

Table 4. TGA Data of the NLO/NSO/NHOSO-DCPD Copolymer Thermosets

NVO-R-DCPD copolymers	$T_{5\%}$	$T_{30\%}$	T_{max}	T_s	residue
NHOSO-DCPD-20	230.4	415.9	471.3	167.4	9.5
NHOSO-DCPD-40	231.8	424.6	474.8	170.3	14.9
NHOSO-DCPD-60	233.2	437.9	476.8	174.4	16.2
NSO-DCPD-20	237.5	425.2	464.2	171.6	9.4
NSO-DCPD-40	246.2	429.5	463.8	174.5	11.4
NSO-DCPD-60	266.4	441.2	470.9	181.9	13.1
NLO-DCPD-20	**294.7**	**445.6**	**454.8**	**188.8**	**13.9**
NLO-DCPD-40	**296.6**	**453.1**	**456.2**	**191.3**	**16.5**
NLO-DCPD-60	**304.2**	**458.1**	**458.9**	**194.3**	**23**

It was demonstrated via TGA analysis that the NLO-DCPD-based thermosets exhibited the best thermal stability as compared to NSO-DCPD and NHOSO-DCPD copolymers. Copolymers with the highest amount of DCPD had the highest residue yields. The T_{max} degradation stage showed that the NHOSO-based thermosets can withstand higher temperature followed by NSO- and NLO-based before undergoing radical degradation. However, the initial weight loss showed the opposite trend and is rather critical in determining an optimum temperature resistance of thermosets to high

temperatures. Statistics index temperatures (T_s) show that the NLO-based thermosets have the highest Ts temperature of 194 °C, followed by NSO (182 °C)- and NHOSO (174 °C)-based thermosets.

The thermo-mechanical properties described earlier in this section (DSC, cross-link efficiency via gel content and TGA) were used as a criterion for selecting the best norbornylized seed oil fit for thermoset applications. NLO-DCPD copolymers were shortlisted for multiple reasons. First, NLO-DCPD copolymers exhibited the highest cross-link efficiency (>67%). Second, even if the difference in the T_g range was minimal in different seed oils, shorter gelation times were exhibited in NLO-DCPD copolymers, presumably due to the higher cure efficiency of NLO during the cationic copolymerization observed in DSC curing data. Third, NLO-DCPD copolymers had the highest thermal stability in terms of the statistics index temperature (T_s) (194 °C), which is critical for any composite application. Thus, only the NLO-DCPD copolymers were made in large numbers to study its tensile properties. The tensile strength of the NLO-DCPD-20 was 4.2 ± 0.9 MPa and tensile modulus was 197 ± 11 MPa. In the thermoset fabrication in large numbers, NLO-DCPD-0 were discarded due to the undesirable tackiness, whereas NLO-DCPD-40 and 60 were discarded because of brittleness. In the next stage, all the variants of shortlisted NLO-DCPD copolymers were reinforced with glass fibers and molded into composites.

3.4. Composite Fabrication and Properties. Composites were molded using the carver press under the same conditions as thermoset. NLO-DCPD copolymers were selected as the base polymer matrix due to the enhanced properties exhibited by its thermosets. NLO-DCPD-0 composites were very tacky probably due to the under cure. This can be attributed to the incorporation of glass fibers affecting the initiator molecule diffusion or chain propagation
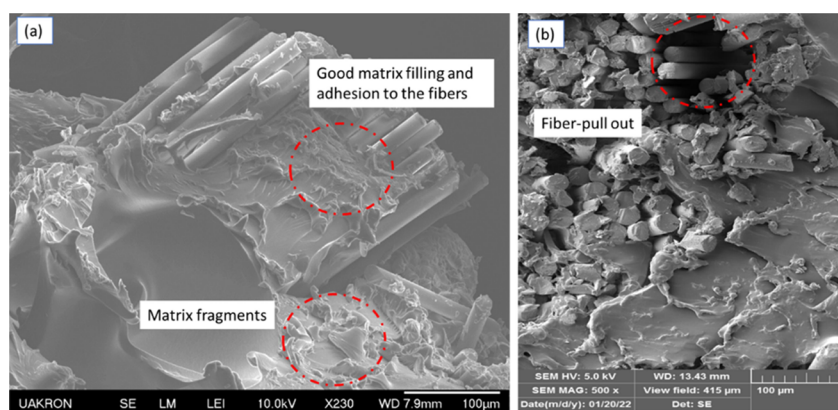
Figure 7. SEM images of fractured surfaces of NLO-DCPD-20 composites at 250× (a) and (b) 500× magnification.

during copolymerization, resulting in lower cross-linking. Furthermore, NLO-DCPD-40 and NLO-DCPD-60 were very brittle and broke down easily on applying pressure. NLO-DCPD-20, however, were good composites with an optimum combination of properties. Thus, NLO-DCPD-20 composites were molded in large numbers for investigating its thermophysical, mechanical, and morphological properties.

Figure 7 shows the cross-sectional SEM images of the fractured surfaces of the composites. As observed from the SEM images, all the composites exhibited two phases corresponding to the polymer matrix and the broken fibers. Residues found adhering on to fiber bundles represents strong bond between the fiber and matrix. As a result of this strong interface adhesion, additional energy might be required to propagate crack causing fiber to break through, and thus, it increases toughness. The shear bands and intensive scraps can be due to the matrix shear yielding followed by a debonding process during the fracture.[73] It can also lead to matrix fragmentation.

Figure 8 shows the DMA data of the NLO-DCPD-20 composites with tan delta and storage modulus data. The
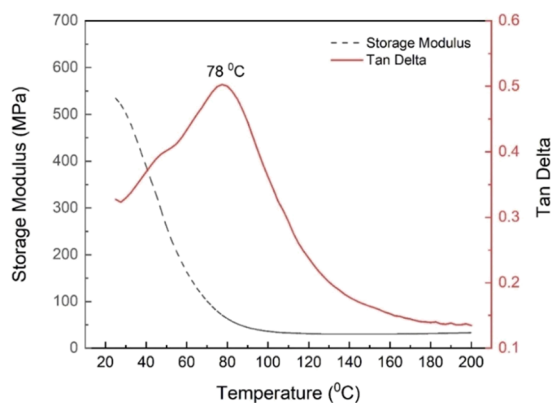
Figure 8. Storage modulus and loss factor (tan delta) for NLO-DCPD-20 composites.

temperature range for the test was from room temperature, below the glass transition temperature, to the polymer composite's rubbery plateau. The amount of elastic energy stored in the sample was indicated by the storage modulus, which correlates to the mechanical and interfacial interaction properties. As seen in Figure 8, storage modulus, indicating the stiffness was observed to be 30 MPa. The peak of tan delta,

representative of T_g exhibited a value of 78 ± 2 °C. DMA T_g is significant, as it is used as both an indication of the upper use temperature of composites and as a quality control aspect.

The TGA thermogram of the NLO-DCPD-20 composites are provided in Figure 9. TGA data of linseed oil, NLO, and
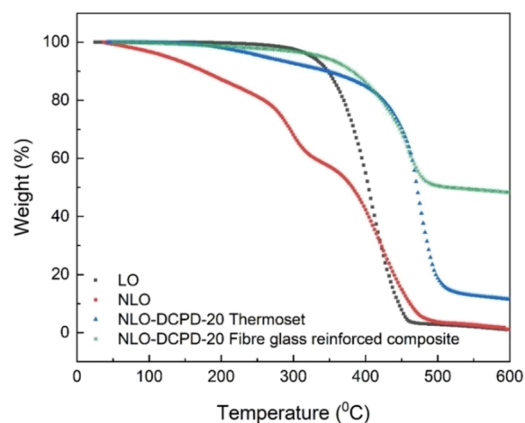
Figure 9. TGA thermogram of LO, NLO, and NLO-DCPD copolymer thermosets and composites.

NLO-DCPD-20 thermosets were also provided for comparison to study the effect of thermal stability from the beginning of the process. Thermal properties throughout the process exhibited distinct enhancement in their thermal behavior. Linseed oil demonstrates a thermal stability of 300 °C, whereas NLO exhibited inferior thermal stability. This observation can be attributed to the presence of residual volatiles in the NLO. Furthermore, DCPD containing polymers is reported to have two degradation steps,[74] a large decomposition temperature is observed in a range of 290−390 °C with T_{max} between 362−365 °C and second degradation at 420−424 °C. In NLO, the presence of DCPD oligomers is evidenced by the degradation peak that start at 290 °C and then again at 400 °C. However, NLO exhibits increased thermal stability after cationic curing with DCPD. In NLO-DCPD copolymer thermosets and composites, the major degradation temperature of 400 °C corresponds to the copolymer. However, there is still degradation observed at 290 °C, which can be due to the DCPD moieties in the copolymer. T_{max} was found to increase by 5% due to the incorporation of glass fibers. However, fiber incorporation also increases the residue content by 30%, followed by NLO-DCPD copolymers, which has 10% residue

lower than NLO. The decrease of residue in the latter case can be attributed to the incorporation of DCPD moieties into the bulk copolymer.

The averaged mechanical property values (5 specimens tested for each sample) are as shown in Table 5. Good tensile

Table 5. Mechanical Properties of NLO-DCPD-20 Composites

types of composite property	NLO-DCPD-20 glass fiber-reinforced composites	standard deviation
tensile strength (MPa)	9	1.4
tensile modulus (MPa)	761	21.3
toughness (J/m^3)	220	11.7
impact strength (J/m)	152	8.2
flexural strength (MPa)	8	1.91
flexural modulus (MPa)	754	19.2

properties suggest good cross-linking, and good flexural properties represent excellent interfacial adhesion between the polymer matrix and the fiber. A higher tensile strength of 42 MPa and Young's modulus of 4 GPa or higher is reported in the case of synthetic glass-reinforced epoxide composites.[75] However, previously reported tensile properties of somewhat comparable bioderived composites show a tensile strength of 10−15 MPa and Young's modulus of 1 GPa.[75,76] NLO-DCPD-20 investigated here exhibited a tensile strength of 9 MPa and Young's modulus of 754 MPa with just 30% fiber glass reinforcement. A similar system with a higher fiber weight percentage (75%) reported Young's modulus of 2.3 GPa.[77,78] The impact properties of biobased glass-reinforced composites have also been investigated and widely reported in the literature, impact strength ranging from 300 J/m by Amal.[79] Yusri et al.[80] reported a flexural strength of 40 MPa on epoxies with hybrid glass/kenaf fiber loading. An exact comparison was not possible because of the changes in the polymer

constituents, and most of the reported literature used more than 50% glass fiber reinforcement, whereas we incorporated no more than 30%.

4. DISCUSSION

Nobornylization of linseed oil and soybean oil has been previously reported by Soucek and co-workers.[18,38,39,42,43,81,82] However, nobornylization of the genetically modified soybean oil, commonly known as the HOSO, is reported here for the first time (27% norbornylization). The investigation of norbornylization of seed oils having different major fatty acid constituents (oleic, linoleic, and linolenic fatty acids) was carried out. A similar amount of unreacted double bonds (2:3) was demonstrated by all seed oils post-norbornylization. Higher norbornylization obtained in NLO is a direct consequence of a higher degree of unsaturation in the linseed oil. At this point, we are not equipped to comment on the direct influence of the different fatty acid constituents on norbornylization. Chances of autoxidation of the seed oil are minimal due to the inert atmosphere maintained throughout the reaction. Furthermore, the absence of homopolymers in the GPC data also rules out the chances of any thermal homopolymerization of seed oil at the high reaction temperature. As a result, higher viscosity can be a direct effect of the higher degree of norbornylization achieved in the seed oil, corroborated by the increased molecular weight.

It is evident that the incorporation of the bicyclic rigid dicyclopentadiene units into the copolymer structure has considerably increased its thermal stability and T_g. DSC characterization study showed NLO to exhibit a higher exotherm during curing owing to the higher number of reactive norbornylized moieties present in it. This observation was corroborated by higher enthalpy, lower activation energy, lower onset, and peak temperature observed in NLO-DCPD copolymers during cationic copolymerization. Higher T_g thermosets were an outcome of the presence of higher norbornene units in the NLO. Furthermore, shorter gelation times of the NLO-DCPD copolymer can also be presumably due to the higher norbornylized constituents present in NLO.

Scheme 3. Illustration of (a) Differences in the Norbornylized Seed Oil Chemical Structure and (b) Chemical Units Responsible for Concomitant Reactions During Cationic Curing in NLO-DCPD
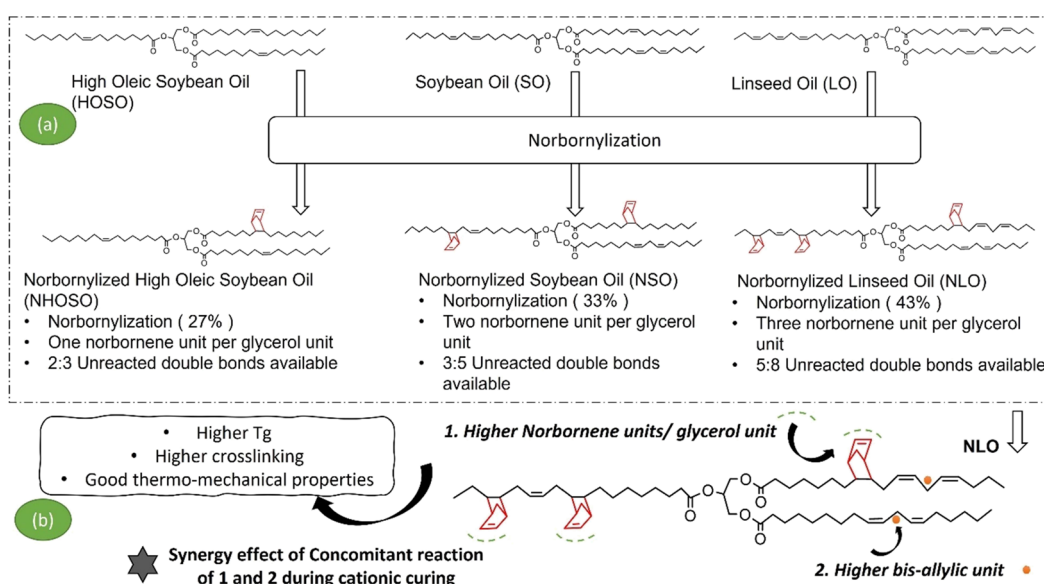
SEM images of the fractured area of the composites showed good polymer matrix adhesion to the fibers and strong interfacial adhesion. As compared to the previous work reported on the thermoset based on cationically cured modified vegetable oil,[47,49,83,84] NLO-DCPD composites demonstrated higher thermal stability, glass transition temperature, and cross-linking capability. The enhancement of properties for the NLO-DCPD composites can be attributed to its better cross-linking. This can be a direct consequence of the synergic effect of higher initial degree of unsaturation, higher norbornene units incorporated, and the simultaneous participation of the bis-allylic unit in the curing process (Scheme 3). The likelihood of any side reactions or free-radical reactions are greatly reduced as the cationic premix-reactions are conducted at room temperature. However, the composite fabrication does require further optimization.

The research elucidates the nobornylization and cationic copolymerization of seed oils primarily constituted by oleic, linoleic, and linolenic fatty acid content. The higher reactivity of the norbornylized seed oil negated the need for any fish oil modifiers otherwise deemed mandatory for a homogeneous copolymer system.[47] Furthermore, a cationically cured norbornylized seed oil-based polymeric matrix system for manufacturing composites has not been previously reported. The thermo-mechanical and morphological results suggests that these materials are feasible alternatives for the current petroleum-based unsaturated polyester composites.[85,86] A biosourced greener copolymer composite is fabricated here to meet the increasing demand for sustainable lightweight material combining superior performance and lesser carbon footprint.

5. CONCLUSIONS

HOSO was norbornylized successfully for the first time. All the norbornylized seed oils demonstrated relatively similar reactive double bond availability. To that extent, higher functionalization via norbornylization in linseed oil was a direct consequence of its higher unsaturation present per glycerol unit. Cationic copolymerization of norbornylized seed oils carried out using dicyclopentadiene units exhibited difference in curing (NLO > NSO > NHOSO). The difference in the degree of unsaturation and content of oleic, linoleic, and linoleic fatty acids between the seed oils strongly influenced the curing and final properties of the copolymers. The concomitant participation of more norbornylized units coupled with the bis-allylic units in linseed oil generated higher T_g NLO-DCPD thermosets. Fabricated NLO-DCPD glass fiber composites also exhibited good interfacial adhesion between the polymer matrix and fiber phases, imparting good thermo-mechanical properties.

ASSOCIATED CONTENT

Ⓢ Supporting Information

The Supporting Information is available free of charge at https://pubs.acs.org/doi/10.1021/acsomega.2c02569.

Details on the Diels−Alder reaction scheme (Scheme S1); characterization of norbornylized seed oils with GPC data (Figure S1); IR spectra (Figure S2) with interpretation of peaks (Table S1); NMR spectra (Figure S3) with interpretation (Section S1); curing study with the reaction scheme (Scheme S2); DSC data of NLO-DCPD curing (Figure S4 and Table S2); GPC

data with interpretation (Figure S5); and NMR spectra (Figure S6) and TGA thermograms (Figure S7) of cured thermosets and composites (PDF)

AUTHOR INFORMATION

Corresponding Author

Mark D. Soucek − *School of Polymer Science and Polymer Engineering, University of Akron, Akron, Ohio 44325, United States;* ⓘ orcid.org/0000-0003-3865-4504; Phone: 330-972-2583; Email: msoucek@uakron.edu

Author

Jomin Thomas − *School of Polymer Science and Polymer Engineering, University of Akron, Akron, Ohio 44325, United States;* ⓘ orcid.org/0000-0003-3783-1898

Complete contact information is available at:
https://pubs.acs.org/10.1021/acsomega.2c02569

Notes

The authors declare no competing financial interest.

REFERENCES

(1) Chamas, A.; Moon, H.; Zheng, J.; Qiu, Y.; Tabassum, T.; Jang, J. H.; Abu-Omar, M.; Scott, S. L.; Suh, S. Degradation Rates of Plastics in the Environment. *ACS Sustainable Chem. Eng.* **2020**, *8*, 3494−3511.

(2) Wandosell, G.; Parra-Meroño, M. C.; Alcayde, A.; Baños, R. Green Packaging from Consumer and Business Perspectives. *Sustainability* **2021**, *13*, 1−19.

(3) Thomas, J. A Methodological Outlook on Bioplastics from Renewable Resources. *Open J. Polym. Chem.* **2020**, *10*, 21−47.

(4) Mohanan, N.; Montazer, Z.; Sharma, P. K.; Levin, D. B. Microbial and Enzymatic Degradation of Synthetic Plastics. *Front. Microbiol.* **2020**, *11*, No. 580709.

(5) Thomas, J.; Moosavian, S. K.; Cutright, T.; Pugh, C.; Soucek, M. D. Investigation of Abiotic Degradation of Tire Cryogrinds. *Polym. Degrad. Stab.* **2022**, *195*, No. 109814.

(6) Namazi, H. Polymers in Our Daily Life. *BioImpacts* **2017**, *7*, 73−74.

(7) Herrera Franco, P. J.; Valadez-González, A. *Fiber-Matrix Adhesion in Natural Fiber Composites*; 2005; DOI: 10.1201/9780203508206.ch6.

(8) Wool, R. P.; Sun, X. S. *Bio-Based Polymers and Composites*; 2005; Vol. *43*, DOI: 10.5860/choice.43-2217.

(9) Coatings, O. *Organic Coatings, Science and Technology*; 1984; Vol. 6.

(10) Alam, M.; Akram, D.; Sharmin, E.; Zafar, F.; Ahmad, S. Vegetable Oil Based Eco-Friendly Coating Materials: A Review Article. *Arabian J. Chem.* **2014**, *7*, 469−479.

(11) Lu, Y.; Larock, R. C. Novel Polymeric Materials from Vegetable Oils and Vinyl Monomers: Preparation, Properties, and Applications. *ChemSusChem* **2009**, *2*, 136−147.

(12) Garrison, T. F.; Murawski, A.; Quirino, R. L. Bio-Based Polymers with Potential for Biodegradability. *Polymers* **2016**, *8*, 1−22.

(13) Mosiewicki, M. A.; Aranguren, M. I. A Short Review on Novel Biocomposites Based on Plant Oil Precursors. *Eur. Polym. J.* **2013**, *49*, 1243−1256.

(14) Meiorin, C.; Aranguren, M. I.; Mosiewicki, M. A. Polymeric Networks Based on Tung Oil: Reaction and Modification with Green Oil Monomers. *Eur. Polym. J.* **2015**, *67*, 551−560.

(15) Thomas, J.; Singh, V.; Jain, R. Synthesis and Characterization of Solvent Free Acrylic Copolymer for Polyurethane Coatings. *Prog. Org. Coat.* **2020**, *145*, No. 105677.

(16) Bao, L.; Bian, L.; Zhao, M.; Lei, J.; Wang, J. Synthesis and Self-Assembly Behavior of a Biodegradable and Sustainable Soybean Oil-Based Copolymer Nanomicelle. *Nanoscale Res. Lett.* **2014**, *9*, 391.

(17) Sain, S.; Åkesson, D.; Skrifvars, M. Synthesis and Properties of Thermosets from Tung Oil and Furfuryl Methacrylate. *Polymers* **2020**, *12*, 258.

(18) Ren, X.; Xu, T.; Soucek, M. *Novel Soy-Based Epoxies for Photopolymerization.*

(19) Petrović, Z. S.; Zhang, W.; Javni, I.; Guo, A. Laminates from the Soy-Based Polyurethanes and Natural and Synthetic Fibers. *Mater. Res. Soc. Symp. Proc.* **2011**, *702*, 141−147.

(20) Allauddin, S.; Somisetti, V.; Ravinder, T.; Rao, B. V. S. K.; Narayan, R.; Raju, K. V. S. N. One-Pot Synthesis and Physicochemical Properties of High Functionality Soy Polyols and Their Polyurethane-Urea Coatings. *Ind. Crops Prod.* **2016**, *85*, 361−371.

(21) Sithique, M. A.; Nagendiran, S.; Alagar, M. Synthesis and Characterization of Bismaleimide-Modified, Soy-Based Epoxy Matrices for Flame-Retardant Applications. *High Perform. Polym.* **2010**, *22*, 328−344.

(22) Barcena, H.; Tuachi, A.; Zhang, Y. Teaching Green Chemistry with Epoxidized Soybean Oil. *J. Chem. Educ.* **2017**, *94*, 1314−1318.

(23) Shafranska, O.; Webster, D. C.; Chisholm, B. J.; McFarlane, S.; Tardiff, J. Modified Soybean Oil as a Processing Oil for Styrene-Butadiene Rubber Tire Tread Compounds. *Tire Sci. Technol.* **2019**, *47*, 280−291.

(24) Frank, J. Flider. *High Oleic Oils: Development, Properties, and Uses*; Elsevier Inc., 2021, DOI: 10.1016/C2019-0-04022-8.

(25) Lamm, M. E.; Li, P.; Hankinson, S.; Zhu, T.; Tang, C. Plant Oil-Derived Copolymers with Remarkable Post-Polymerization Induced Mechanical Enhancement for High Performance Coating Applications. *Polymer* **2019**, *174*, 170−177.

(26) Podolsky, J.; Hohmann, A.; Chen, C.; Sotoodeh-Nia, Z.; Manke, N.; Saw, B.; Hernandez, N.; Ledtje, P.; Forrester, M.; Christopher Williams, R.; Cochran, E.; Huisman, T. *Effect of Soybean Oil Derived Additives on Improved Performance of Polymer-Modified Asphalt Binder and Mix Containing 50% Fine-Graded RAP*. Springer International Publishing 2022; Vol. 27, DOI: 10.1007/978-3-030-46455-4_78.

(27) Karak, N. Overview of Epoxies and Their Thermosets. *ACS Symp. Ser.* **2021**, *1385*, 1−36.

(28) Tran, T. N.; Di Mauro, C.; Graillot, A.; Mija, A. Chemical Reactivity and the Influence of Initiators on the Epoxidized Vegetable Oil/Dicarboxylic Acid System. *Macromolecules* **2020**, *53*, 2526−2538.

(29) Vadiraj, J. H.; Vikas, R. S.; Zade, P. S.; Mandake, M. B.; Walke, S. Review: Epoxidation of Vegetable Oils. *Int. J. Trend Res. Dev.* **2018**, *5*, 542−548.

(30) Phillip Henna, R. C. L. Novel Thermosets Obtained by the Ring-Opening Metathesis Polymerization of a Functionalized Vegetable Oil and Dicyclopentadiene. *J. Appl. Polym. Sci.* **2009**, *112*, 1788−1797.

(31) Miyagawa, H.; Misra, M.; Drzal, L. T.; Mohanty, A. K. Fracture Toughness and Impact Strength of Anhydride-Cured Biobased Epoxy. *Polym. Eng. Sci.* **2005**, *45*, 487−495.

(32) Sharmin, E.; Zafar, F.; Akram, D.; Alam, M.; Ahmad, S. Recent Advances in Vegetable Oils Based Environment Friendly Coatings: A Review. *Ind. Crops Prod.* **2015**, *76*, 215−229.

(33) Eom, H. S. *Photopolymerizations of Multicomponent Epoxide and Acrylate/Epoxide Hybrid Systems for Controlled Kinetics and Enhanced Material Properties*, 2011.

(34) Zong, Z.; He, J.; Soucek, M. D. UV-Curable Organic-Inorganic Hybrid Films Based on Epoxynorbornene Linseed Oils. *Prog. Org. Coat.* **2005**, *53*, 83−90.

(35) Bellville, D. J.; Bauld, N. L. Selectivity Profile of the Cation Radical Diels-Alder Reaction. *J. Am. Chem. Soc.* **1982**, *104*, 2665−2667.

(36) Bellville, D. J.; Wirth, D. D.; Bauld, N. L. The Cation-Radical Catalyzed Diels-Alder Reaction. *J. Am. Chem. Soc.* **1981**, *103*, 718−720.

(37) Kulkosky, P. F. Linseed oil based polymeric vehicle. US Patent 5288805, 1994, DOI: 10.1016/0163-7258(94)90062-0.

(38) Chen, J.; Soucek, M. D.; Simonsick, W. J.; Celikay, R. W. Synthesis and Photopolymerization of Norbornyl Epoxidized Linseed Oil. *Polymer* **2002**, *43*, 5379−5389.

(39) Li, J.; Isayev, A. I.; Ren, X.; Soucek, M. D. Norbornylized Soybean Oil as a Sustainable New Plasticizer for Rubbers with Hybrid Fillers. *Polym. Int.* **2017**, *66*, 820−829.

(40) Zou, K.; Soucek, M. D. UV-Curable Cycloaliphatic Epoxide Based on Modified Linseed Oil: Synthesis, Characterization and Kinetics. *Macromol. Chem. Phys.* **2005**, *206*, 967−975.

(41) Teng, G.; Soucek, M. D. Epoxidized Soybean Oil-Based Ceramer Coatings. *J. Am. Oil Chem. Soc.* **2000**, *77*, 381−387.

(42) Ren, X.; Xu, T.; Thomas, J.; Soucek, M. D. Isoprene Soya Diels−Alder Adduct and Epoxidation for Photopolymerization. *Macromol. Chem. Phys.* **2021**, *222*, 1−11.

(43) Li, J.; Isayev, A. I.; Ren, X.; Soucek, M. D. Effect of Norbornyl Modified Soybean Oil on CB-Filled Chloroprene Rubber. *J. Appl. Polym. Sci.* **2016**, *133*, 43809.

(44) Mauldin, T. C.; Haman, K.; Sheng, X.; Henna, P.; Larock, R. C.; Kessler, M. R. Ring-Opening Metathesis Polymerization of a Modified Linseed Oil with Varying Levels of Crosslinking. *J. Polym. Sci., Part A: Polym. Chem.* **2008**, *46*, 6851−6860.

(45) Quirino, R. L.; Ma, Y.; Larock, R. C. Oat Hull Composites from Conjugated Natural Oils. *Green Chem.* **2012**, *14*, 1398−1404.

(46) Kundu, P. P.; Larock, R. C. Novel Conjugated Linseed Oil-Styrene-Divinylbenzene Copolymers Prepared by Thermal Polymerization. 1. Effect of Monomer Concentration on the Structure and Properties. *Biomacromolecules* **2005**, *6*, 797−806.

(47) Andjelkovic, D. D.; Larock, R. C. Novel Rubbers from Cationic Copolymerization of Soybean Oils and Dicyclopentadiene. 1. Synthesis and Characterization. *Biomacromolecules* **2006**, *7*, 927−936.

(48) Xia, Y.; Larock, R. C. Vegetable Oil-Based Polymeric Materials: Synthesis, Properties, and Applications. *Green Chem.* **2010**, *12*, 1893−1909.

(49) Lu, Y.; Larock, R. C. Corn Oil-Based Composites Reinforced with Continuous Glass Fibers: Fabrication and Properties. *J. Appl. Polym. Sci.* **2006**, *102*, 3345−3353.

(50) Li, F.; Larock, R. C. New Soybean Oil-Styrene-Divinylbenzene Thermosetting Copolymers. I. Synthesis and Characterization. *J. Appl. Polym. Sci.* **2001**, *80*, 658−670.

(51) Hummer, C. C. Natural Oil-Based Composites Reinforced with Natural Fillers, and Conjugation/Isomerization of Carbon-Carbon Double Bonds. *Biface Ceram. Assem. Var. Early Woodl. Contin. Chang. Williamson Site, Hunterdon County, New Jersey*, 1991.

(52) Del Saz-Orozco, B.; Alonso, M. V.; Oliet, M.; Domínguez, J. C.; Rodriguez, F. Mechanical, Thermal and Morphological Characterization of Cellulose Fiber-Reinforced Phenolic Foams. *Composites, Part B* **2015**, *75*, 367−372.

(53) Advani, S. G.; Hsiao, K. T. *Manufacturing Techniques for Polymer Matrix Composites (PMCs)*; 2012, DOI: 10.1533/9780857096258.

(54) Samarth, N. B.; Mahanwar, P. A. Modified Vegetable Oil Based Additives as a Future Polymeric Material—Review. *Open J. Org. Polym. Mater.* **2015**, *05*, 1−22.

(55) Wang, R. Manufacturing of Vegetable Oils-Based Epoxy and Composites for Structural Applications. *Missouri Univ. Sci. Technol.* **2014**, 5−10.

(56) Kulshreshtha, A. K. *Handbook of Polymer Blends and Composites, Volume 1*; 2002; Vol. 1.

(57) Patil, R. S.; Sancaktar, E. Fabrication of PH-Responsive Polyimide Polyacrylic Acid Smart Gating Membranes: Ultrafast

Method Using 248 Nm Krypton Fluoride Excimer Laser. *ACS Appl. Mater. Interfaces* **2021**, 24431.

(58) Briou, B.; Améduri, B.; Boutevin, B. Trends in the Diels-Alder Reaction in Polymer Chemistry. *Chem. Soc. Rev.* **2021**, *50*, 11055−11097.

(59) Xia, Y.; Henna, P. H.; Larock, R. C. Novel Thermosets from the Cationic Copolymerization of Modified Linseed Oils and Dicyclopentadiene. *Macromol. Mater. Eng.* **2009**, *294*, 590−598.

(60) Andjelkovic, D. D.; Valverde, M.; Henna, P.; Li, F.; Larock, R. C. Novel Thermosets Prepared by Cationic Copolymerization of Various Vegetable Oils - Synthesis and Their Structure-Property Relationships. *Polymer* **2005**, *46*, 9674−9685.

(61) Armylisasa, A. H. N.; Hazirahb, M. F. S.; Yeonga, S. K.; Hazimaha, A. H. Modification of Olefinic Double Bonds of Unsaturated Fatty Acids and Other Vegetable Oil Derivatives via Epoxidation: A Review. *Grasas Aceites* **2017**, *68*, 1−11.

(62) Sacchi, R.; Addeo, F.; Paolillo, L. 1H and 13C NMR of Virgin Olive Oil. An Overview. *Magn. Reson. Chem.* **1997**, *35*, S133−S145.

(63) Aerts, H. A. J.; Jacobs, P. A. Epoxide Yield Determination of Oils and Fatty Acid Methyl Esters Using 1H NMR. *J. Am. Oil Chem. Soc.* **2004**, *81*, 841−846.

(64) Rueter, P.; Rabus, R.; Wilkest, H.; Aeckersberg, F.; Rainey, F. A.; Jannasch, H. W.; Widdel, F. Anaerobic Oxidation of Hydrocarbons in Crude Oil by New Types of Sulphate-Reducing Bacteria. *Nature* **1994**, *372*, 455−458.

(65) Matyjaszewski. *Cationic Polymerization: Mechanisms, Synthesis and Applications*; Marcel Dekker: New York, 1996.

(66) Fink, J. . *Reactive Polymers Fundamentals and Applications: A Concise Guide to Industrial Polymers*; William andrew publishing: New York, 2005.

(67) Henna, P. H.; Kessler, M. R.; Larock, R. C. Fabrication and Properties of Vegetable-Oil-Based Glass Fiber Composites by Ring-Opening Metathesis Polymerization. *Macromol. Mater. Eng.* **2008**, *293*, 979−990.

(68) Zanchin, G.; Leone, G.; Pierro, I.; Rapallo, A.; Porzio, W.; Bertini, F.; Ricci, G. Addition Oligomerization of Dicyclopentadiene: Reactivity of Endo and Exo Isomers and Postmodification. *Macromol. Chem. Phys.* **2017**, *218*, 1−8.

(69) Rule, J. D.; Moore, J. S. ROMP Reactivity of Endo- and Exo-Dicyclopentadiene. *Macromolecules* **2002**, *35*, 7878−7882.

(70) Kovačič, S.; Slugovc, C. Ring-Opening Metathesis Polymerisation Derived Poly(Dicyclopentadiene) Based Materials. *Mater. Chem. Front.* **2020**, *4*, 2235−2255.

(71) Peng, Y. X.; Liu, J. L.; Cun, L. F. Microstructure of Polymers Obtained by Cationic Polymerization of Endo-Dicyclopentadiene. *J. Polym. Sci., Part A: Polym. Chem.* **1996**, *34*, 3527−3530.

(72) Badrinarayanan, P.; Lu, Y.; Larock, R. C.; Kessler, M. R. Cure Characterization of Soybean Oil—Styrene—Divinylbenzene Thermosetting Copolymers. *J. Appl. Polym. Sci.* **2009**, *113*, 1042−1049.

(73) Saravanakumar, K.; Arumugam, V.; Souhith, R.; Santulli, C. Influence of Milled Glass Fiber Fillers on Mode I & Mode II Interlaminar Fracture Toughness of Epoxy Resin for Fabrication of Glass/Epoxy Composites. *Fibers* **2020**, *8*, 36.

(74) O'Donnell, A.; Dweib, M. A.; Wool, R. P. Natural Fiber Composites with Plant Oil-Based Resin. *Compos. Sci. Technol.* **2004**, *64*, 1135−1145.

(75) Manthey, N. W.; Cardona, F.; Francucci, G.; Aravinthan, T. Thermo-Mechanical Properties of Epoxidized Hemp Oil-Based Bioresins and Biocomposites. *J. Reinf. Plast. Compos.* **2013**, *32*, 1444−1456.

(76) Liu, Z.; Erhan, S. Z.; Akin, D. E.; Barton, F. E. "Green" Composites from Renewable Resources: Preparation of Epoxidized Soybean Oil and Flax Fiber Composites. *J. Agric. Food Chem.* **2006**, *54*, 2134−2137.

(77) Chandrashekhara, K.; Sundararaman, S.; Flanigan, V.; Kapila, S. Affordable Composites Using Renewable Materials. *Mater. Sci. Eng., A* **2005**, *412*, 2−6.

(78) Boquillon, N. Use of an Epoxidized Oil-Based Resin as Matrix in Vegetable Fibers-Reinforced Composites. *J. Appl. Polym. Sci.* **2006**, *101*, 4037−4043.

(79) Badawy, A. A. M. Impact Behavior of Glass Fibers Reinforced Composite Laminates at Different Temperatures. *Ain Shams Eng. J.* **2012**, *3*, 105−111.

(80) Muhammad, Y. H.; Ahmad, S.; Abu Bakar, M. A.; Mamun, A. A.; Heim, H. P. Mechanical Properties of Hybrid Glass/Kenaf Fibre-Reinforced Epoxy Composite with Matrix Modification Using Liquid Epoxidised Natural Rubber. *J. Reinf. Plast. Compos.* **2015**, *34*, 896−906.

(81) Chen, J.; Soucek, M. D.; Simonsick, W. J.; Celikay, R. W. Epoxidation of Partially Norbornylized Linseed Oil. *Macromol. Chem. Phys.* **2002**, *203*, 2042−2057.

(82) Zong, Z.; Soucek, M. D.; Liu, Y.; Hu, J. Cationic Photopolymerization of Epoxynorbornane Linseed Oils: The Effect of Diluents. *J. Polym. Sci., Part A: Polym. Chem.* **2003**, *41*, 3440−3456.

(83) Lu, Y.; Larock, R. C. Novel Biobased Plastics, Rubbers, Composites, Coatings and Adhesives from Agricultural Oils and by-Products. *ACS Symp. Ser.* **2010**, *1043*, 87−102.

(84) Kalita, D. J.; Tarnavchyk, I.; Sibi, M.; Moser, B. R.; Webster, D. C.; Chisholm, B. J. Biobased Poly(Vinyl Ether)s Derived from Soybean Oil, Linseed Oil, and Camelina Oil: Synthesis, Characterization, and Properties of Crosslinked Networks and Surface Coatings. *Prog. Org. Coat.* **2018**, *125*, 453−462.

(85) Wu, Y.; Fei, M.; Qiu, R.; Liu, W.; Qiu, J. A Review on Styrene Substitutes in Thermosets and Their Composites. *Polymers* **2019**, *11*, 1815.

(86) Fernandes, F. C.; Kirwan, K.; Wilson, P. R.; Coles, S. R. Sustainable Alternative Composites Using Waste Vegetable Oil Based Resins. *J. Polym. Environ.* **2019**, *27*, 2464−2477.